Supplementary Information

Limited effects of different real groundwaters from three coastal cities in China on the transport of low-concentration nanoplastics in quartz sand

Yanan Liu[a], Genyao Gu[a], Guoqing Li[a], Hyunjung Kim[b], Li Cai[a, *], Huiwen Cai[c, *]

[a] College of Environmental Science and Engineering, Donghua University, Shanghai 201620, P. R. China

[b] Department of Earth Resources and Environmental Engineering, Hanyang University, 222 Wangsimni-ro, Seongdong-gu, Seoul 04763, Republic of Korea

[c] Takuvik, CNRS/Université Laval, IRL3376, 1045 avenue de la, Médecine Quebec QC, G1V0A6, Canada

[*]Corresponding author. E-mail: caili@dhu.edu.cn (Cai L.,); E-mail: huiwen.cai93@gmail.com (Cai H. W.,).

Number of Pages: 11

Number of Tables: 2

Number of Figures: 3

Text S1. NPs concentration determination

The concentration of both PS and PLGA NPs were analyzed using a fluorescence spectrophotometer (F7000, Hitachi, Japan) with 10 mm × 10 mm quartz cuvette. The optimum excitation/emission wavelengths to detect the PS NPs (both 0.51 and 1.1 μm) and PLGA NPs were determined to be 468/508 nm and 460/500 nm, respectively, and the excitation and emission slits of the instrument were both set at 5 nm. The calibration results confirmed a linear correlation between the NPs concentration and the intensity of the fluorescence signals over the range of the investigated NPs concentrations (Fig. S2). To testify the influence of real groundwaters on the detection of NP using fluorescence spectrophotometer, NPs suspension diluted with both DI water and real groundwater samples (ZJ site) at the same concentration were prepared. Then, the concentrations of samples were determined by fluorescence spectrophotometer, and the results were presented in Fig. S3. It was observed that the detected concentration of NPs were equal in DI waters and groundwater, indicating the negligible influence of real groundwaters on the detection of NPs using fluorescence spectrophotometer.

Text S2. Column experiments protocol

Ultrapure quartz sand (Minghai Quartz Sand Factory, Zhengzhou, China) with sizes ranging from 417 to 600 μm was as porous media for the NPs transport experiments. The quartz sand was cleaned by soaking in concentrated HCl for at least 24 hours, and then in 1 M NaOH solution for another 24 hours. After acid-washing and

alkali-washing, the quartz sand was washed with DI water repeatedly to bring the pH to neutral. Then the quartz sand was dried at 105 °C overnight, and then baking overnight at 850 °C for at least 8 h.

Prior to packing, the cleaned quartz sand was rehydrated by boiling in DI water for at least 0.5 h. After the rehydrated quartz sand was cooled, the columns were packed by adding wet quartz sand in small increments (~ 1 cm) with mild vibration of the column to minimize any layering or air entrapment. One 80 mesh fabric screen was placed at each end of the column.

Text S3. Calculation of interaction energies between NPs-NPs and NPs-sand

The Derjaguin-Landau-Verwey-Overbeek (DLVO) theory was used to calculate the interaction energies (V_{TOT}), a sum of van der Waals (V_{VDW}) and electrostatic double layer (V_{EDL}) interactions, between NPs and NPs (sphere to sphere).

$$V_{TOT} = V_{VDW} + V_{EDL}$$

The van der Waals interaction is calculated by [1]

$$V_{VDW} = -\frac{Aa}{12h}$$

where A is the Hamaker constant for NPs (1.0×10^{-20} J for PS [2, 3] and 6.0×10^{-21} J for PLGA [4]), a is the radius of NPs (m), and h is the separation distance between NPs and NPs (m).

The electronics double layer interaction is calculated by

$$V_{EDL} = 32\pi a \left(\frac{k_B T}{ze}\right)^2 \gamma^2 e^{(-\kappa h)}$$

where k_B is Boltzmann constant (1.38×10^{-23} J/K), T is the Kevin temperature (298 K), z is the indifferent ion valence (treated as 1 in this study), e is the elementary charge (1.6×10^{-19} C), and κ is the Debye length (m^{-1}), defined as

$$k = \sqrt{\frac{2N_A e^2 I}{\varepsilon_r \varepsilon_0 k_B T}}$$

and γ is a dimensionless function of the surface potential, defined as

$$\gamma = \tanh\left(\frac{ze\varphi}{4k_B T}\right)$$

where N_A is Avogadro's number (6.02×10^{23} mol^{-1}), I is the ionic strength of the real groundwaters (converted from the conductivities of the real groundwaters, 12.88 mS/cm treated as 0.1 mM IS), ε_0 is the permittivity in vacuum (8.85×10^{-12} C^2/J m), ε_r is the relative dielectric permittivity of water (78.4), and φ is the surface charge, approximated by the zeta-potentials of NPs.

We used the extended DLVO (XDLVO) theory to calculate the interaction energies (V'_{TOT}) between NPs and sand (sphere to plate). It includes V'_{VDW}, V'_{EDL}, and Lewis acid-base (V_{AB}) interaction. The van der Waals interaction is calculated by

$$V'_{VDW} = -\frac{Ar}{6h\left(1 + \frac{14h}{\lambda}\right)}$$

where h is the separation distance between NPs and sand, and λ is the characteristic wavelength (42.5 nm) [5].

The electrostatic double layer interaction is calculated by

$$V_{EDL} = \pi r \varepsilon_0 \varepsilon_r \left\{ 2\phi_1 \phi_2 \ln\left[\frac{1 + \exp(-kh)}{1 - \exp(-kh)}\right] + (\phi_1^2 + \phi_2^2)\ln[1 - \exp(-2kh)] \right\}$$

where ϕ_1 and ϕ_2 are the surface potentials of NPs and sand, respectively.

The Lewis acid-base (V_{AB}) interaction energy is calculated by

$$V_{AB} = 2\pi r \lambda_w \Delta G_{h_0}^{AB} \exp\left(\frac{h_0 - h}{\lambda_w}\right)$$

where λ_w is the characteristic decay length (0.6 nm) of acid-base interactions in water [6], h_0 is the minimum equilibrium distance (0.157 nm) between NPs and sand surface [6], and $\Delta G_{h_0}^{AB}$ can be calculated as:

$$\Delta G_{h_0}^{AB} = 2\left[\sqrt{\gamma_w^+}\left(\sqrt{\gamma_m^-} + \sqrt{\gamma_s^-} - \sqrt{\gamma_w^-}\right) + \sqrt{\gamma_w^-}\left(\sqrt{\gamma_m^+} + \sqrt{\gamma_s^+} - \sqrt{\gamma_w^+}\right) - \sqrt{\gamma_m^-\gamma_s^+} - \sqrt{\gamma_m^+\gamma_s^-}\right]$$

where the subscripts *m*, *w* and *s* represent NPs, water and sand, respectively, electron Υ^+ (Υ^-) is the electronics accepting (donating) interfacial tension ($\gamma_w^+ = \gamma_w^- = 25.5$ mJ/m^2, $\gamma_s^+ = 1.4$ mJ/m^2, $\gamma_s^- = 47.8$ mJ/m^2, $\gamma_m^+ = 0.02$ mJ/m^2, and $\gamma_m^- = 7.6$ mJ/m^2) [7, 8].

Table S1. Breakthrough mass recovery of column experiments.

NPs	Site	Breakthrough mass recovery (%)
PS, 0.51 μm	FJ	91.21±1.08
	ZJ	91.67±3.71
	JS	80.07±1.60
PS, 1.1 μm	FJ	87.66±1.61
	ZJ	88.60±1.69
	JS	90.30±0.96
PLGA, 1 μm	FJ	22.62±0.52
	ZJ	27.80±3.26
	JS	31.15±0.20

Table S2. Zeta potentials of NPs and quartz sand, and average sizes of NPs with different real groundwaters.

NPs and sand	Site	Zeta potential (mV)	Average size (nm)
PS, 0.51 μm	FJ	-41.32±2.35	771.40±39.99
	ZJ	-16.88±1.95	635.85±3.18
	JS	-19.93±0.92	670.87±14.21
PS, 1.1 μm	FJ	-34.27±0.58	3220.32±96.28
	ZJ	-13.96±0.27	1119.26±13.34
	JS	-15.5±0.59	1205.91±73.16
PLGA, 1 μm	FJ	-8.06±1.65	18168.64±1072.73
	ZJ	-11.03±1.96	24716.84±3042.68
	JS	-5.31±2.20	24819.29±4189.81
Quartz sand	FJ	-25.52±0.37	NA
	ZJ	-13.69±1.95	
	JS	-17.51±0.43	

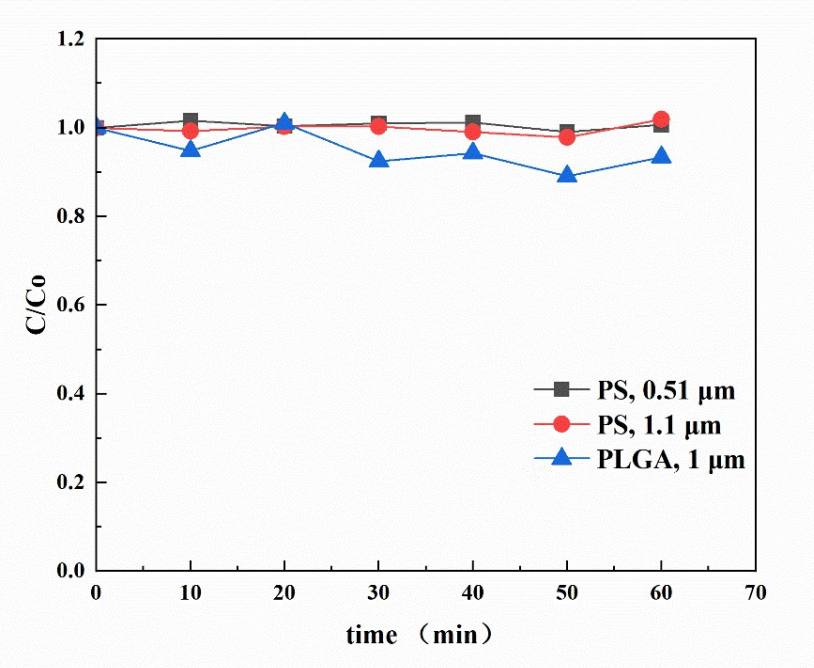

78

79 **Fig. S1.** The stability of both PS and PLGA NPs in DI water.

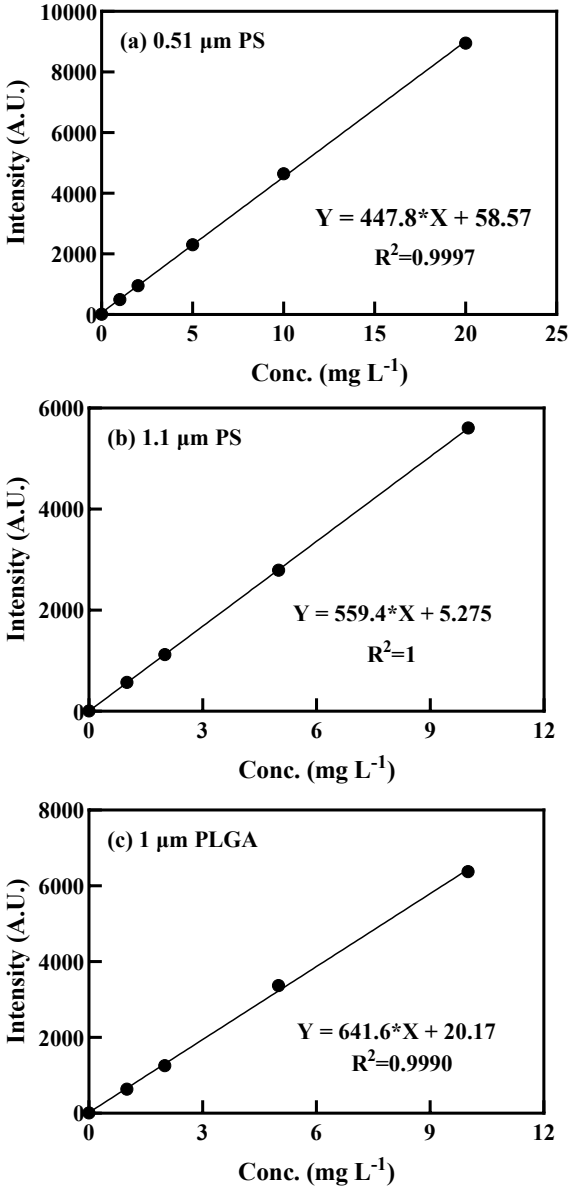

80

81 **Fig. S2.** Calibration curves of PS and PLGA NPs with fluorescence spectrophotometer.

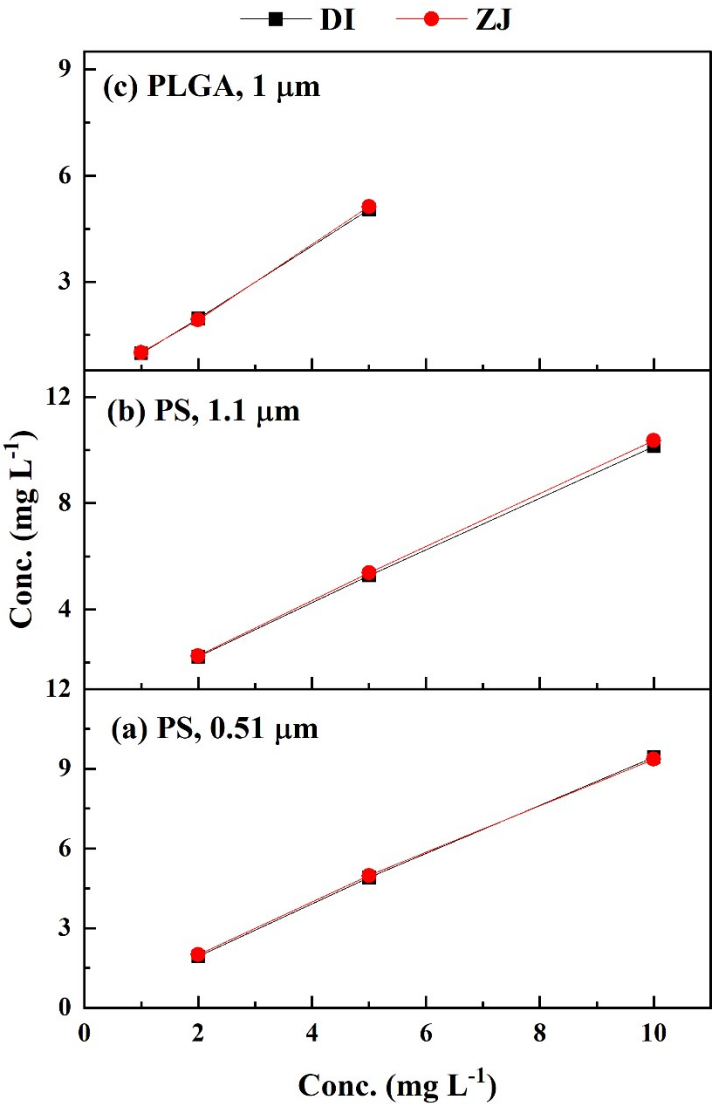

82

83 **Fig. S3.** Influence of groundwater on the detection of NPs using fluorescence

84 spectrophotometer.

References

1. M. Elimelech, J. Gregory, X. Jia and R. A. F. Williams, *Particle Deposition and Aggregation*, 1995.
2. K. Gotoh, R. Kohsaka, K. Abe and M. Tagawa, Estimation of the Hamaker constant from flocculation in the secondary minimum and its experimental verification in particle adhesion, J. Adhes. Sci. Technol., 1996, 10, 1359-1370.
3. M. B. Seymour, G. Chen, C. Su and Y. Li, Transport and retention of colloids in porous media: Does shape really matter?, *Environ. Sci. Technol.*, 2013, 47, 8391-8398.
4. J. Fei, H. Xie, Y. Zhao, X. Zhou, H. Sun, N. Wang, J. Wang and X. Yin, Transport of degradable/nondegradable and aged microplastics in porous media: Effects of physicochemical factors, *Sci. Total Environ.*, 2022, 851, 158099.
5. L. Suresh and J. Y. Walz, Effect of Surface Roughness on the interaction energy between a colloidal sphere and a flat plate, *J. Colloid. Interf. Sci.*, 1996, 183, 199-213.
6. T. Xia, J. D. Fortner, D. Zhu, Z. Qi and W. Chen, Transport of sulfide-reduced graphene oxide in saturated quartz sand: Cation-dependent retention mechanisms, *Environ. Sci. Technol.*, 2015, 49, 11468-11475.
7. A. M. Gallardo-Moreno, M. L. Gonzalez-Martin, C. Perez-Giraldo, E. Garduno, J. M. Bruque and A. C. Gomez-Garcia, Thermodynamic analysis of growth temperature dependence in the adhesion of *Candida parapsilosis* to polystyrene, *Appl. Environ. Microb.*, 2002, 68, 2610-2613.
8. Y. Sun, B. Gao, S. A. Bradford, L. Wu, H. Chen, X. Shi and J. Wu, Transport, retention, and size perturbation of graphene oxide in saturated porous media: effects of input concentration and grain size, *Water Res.*, 2015, 68, 24-33.